Inorg. Chem. **2006**, *45*, 5018–5026

Synthesis, Structures, and Magnetic Properties of a Series of Cyano-Bridged Fe–Mn Bimetallic Complexes

Long Jiang,[†] Xiao-Long Feng,[†] Tong-Bu Lu,*[,†] and Song Gao*[,‡]

State Key Laboratory of Optoelectronic Materials and Technologies and School of Chemistry and Chemical Engineering, Sun Yat-Sen University, Guangzhou 510275, China, and Beijing National Laboratory for Molecular Sciences, State Key Laboratory of Rare Earth Materials Chemistry and Application, College of Chemistry, Peking University, Beijing 100871, China

Received December 21, 2005

The preparation and crystal structures of five cyano-bridged Fe–Mn complexes, $[(bipy)_2Fe^{II}(CN)_2Mn^{II}(bipy)_2]_2(ClO_4)_4$ (**1**), $[(bipy)_2Fe^{II}(CN)_2Mn^{II}(DMF)_3(H_2O)]_2(ClO_4)_4$ (**2**), $\{[(Tp)Fe^{III}(CN)_3]_2Mn^{II}(DMF)_2(H_2O)\}_2$ (**3**), $\{[(Tp)Fe^{III}(CN)_3]_2Mn^{II}(DMF)_2\}_n$ (**4**), and $Na_2[Mn^{II}Fe^{II}(CN)_6]$ (**5**) (bipy = 2,2′-bipyridine, Tp = tris(pyrazolyl)hydroborate), are reported here. Compounds **1**–**4** contain the basic $Fe_2(CN)_4Mn_2$ square building units, of which **1**–**3** show the motif of discrete molecular squares of $Fe_2(CN)_4Mn_2$ and **4** possesses a 1D double-zigzag chainlike structure, while compound **5** is a 3D cubic framework analogous to that of Prussian blue. Compounds **1** and **2** show weak ferromagnetic interactions between two Mn(II) ions through the bent –NC–Fe(II)–CN– bridges. Compound **3** shows weak antiferromagnetic coupling between the Fe(III) and Mn(II) ions, while compound **4** displays a metamagnetic-like behavior with T_N = 5.2 K and H_c = 10.5 kOe. Compound **5** exhibits a ferromagnetic ordering with T_c = 3.5 K, coercive field, H_c, = 330 G, and a remnant magnetization of 503 cm^3 Oe mol^{-1}.

Introduction

Cyano-bridged clusters[1] and coordination polymers[2−9] have been extensively investigated in the field of molecular magnetism because the cyano bridge can be an efficient propagation for magnetic coupling. Indeed, most of the known molecule-based magnets with T_c values above room temperature, such as $V^{II}_{0.42}V^{III}_{0.58}[Cr^{III}(CN)_6]_{0.86}\cdot 2.8H_2O$ (T_c = 315 K),[2a] $K_{0.058}V[Cr^{III}(CN)_6]_{0.79}(SO_4)_{0.058}\cdot 0.93H_2O$ (T_c = 372 K),[2b] and $KV[Cr^{III}(CN)_6]\cdot 2H_2O$ (T_c = 376 K),[2c] belong to the cyano-bridged Prussian blue family. However, the origin of the high T_c remains unclear because of the lack of structural information. To better understand the magneto-structural relationship, some cyano-bridged bimetallic as-

* To whom correspondence should be addressed. E-mail: cesltb@zsu.edu.cn (T.-B.L.); gaosong@pku.edu.cn (G.S.).
† Sun Yat-Sen University.
‡ Peking University.

(1) Beltran, L. M. C.; Long, J. R. *Acc. Chem. Res.* **2005**, *38*, 325. (b) Beauvais, L. G.; Long, J. R. *J. Am. Chem. Soc.* **2002**, *124*, 12096. (c) Berben, L. A.; Long, J. R. *J. Am. Chem. Soc.* **2002**, *124*, 11588. (d) Sokol, J. J.; Hee, A. G.; Long, J. R. *J. Am. Chem. Soc.* **2002**, *124*, 7656. (e) Shores, M. P.; Sokol, J. J.; Long, J. R. *J. Am. Chem. Soc.* **2002**, *124*, 2279. (f) Beauvais, L. G.; Long, J. R. *J. Am. Chem. Soc.* **2002**, *124*, 2110. (g) Sokol, J. J.; Shores, M. P.; Long, J. R. *Inorg. Chem.* **2002**, *41*, 3052. (h) Sokol, J. J.; Shores, M. P.; Long, J. R. *Angew. Chem., Int. Ed. Engl.* **2001**, *40*, 236. (i) Berseth, P. A.; Sokol, J. J.; Shores, M. P.; Heinrich, J. L.; Long, J. R. *J. Am. Chem. Soc.* **2000**, *122*, 9655. (j) Larionova, J.; Gross, M.; Pilkington, M.; Andres, H.; Stoeckli-Evans, H.; Güdel, H. U.; Decurtins, S. *Angew. Chem., Int. Ed.* **2000**, *39*, 1605. (k) Chen, X. Y.; Shi, W.; Xia, J.; Cheng, P.; Zhao, B.; Song, H. B.; Wang, H. G.; Yan, S. P.; Liao, D. Z.; Jiang, Z. H. *Inorg. Chem.* **2005**, *44*, 4263. (l) Ni, Z. H.; Kou, H. Z.; Zhao, Y. H.; Wang, R. J.; Cui, A. L.; Sato, O. *Inorg. Chem.* **2005**, *44*, 2050. (m) Choi, H. J.; Sokol, J. J.; Long, J. R. *Inorg. Chem.* **2004**, *43*, 1606.

(2) Ferlay, S.; Mallah, T.; Ouahes, R.; Veillet, P.; Verdaguer, M. *Nature* **1995**, *378*, 701. (b) Hatlevik, Ø.; Buschmann, W. E.; Zhang, J.; Manson, J. L.; Miller, J. S. *Adv. Mater.* **1999**, *11*, 914. (c) Holmes, S. M.; Girolami, G. S. *J. Am. Chem. Soc.* **1999**, *121*, 5593. (d) Lu, T. B.; Xiang, H.; Su, C. Y.; Cheng, P.; Mao, Z. W.; Ji, L. N. *New J. Chem.* **2001**, *25*, 216.

(3) Inoue, K.; Imai, H.; Chalsasi, P. S.; Kikuchi, K.; Ohba, M.; Ôkawa, H.; Yakhmi, J. V. *Angew. Chem., Int. Ed.* **2001**, *40*, 4242.

(4) Kou, H. Z.; Gao, S.; Zhang, J.; Wen, G. H.; Su, G.; Zheng, R. K.; Zhang, X. X. *J. Am. Chem. Soc.* **2001**, *123*, 11809.

(5) Dong, W.; Zhu, L. N.; Song, H. B.; Liao, D. Z.; Jiang, Z. H.; Yan, S. P.; Cheng, P.; Gao, S. *Inorg. Chem.* **2004**, *43*, 2465.

(6) Ohba, M.; Usuki, N.; Fukita, N.; Ôkawa, H. *Angew. Chem., Int. Ed.* **1999**, *38*, 1795.

(7) Tanase, S.; Tuna, F.; Guionneau, P.; Maris, T.; Rombaut, G.; Mathoniere, C.; Andruh, M.; Kahn, O.; Sutter, J. *Inorg. Chem.* **2003**, *42*, 1625.

(8) Shores, M. P.; Beauvais, L. G.; Long, J. R. *J. Am. Chem. Soc.* **1999**, *121*, 775.

(9) Nihei, M.; Ui, M.; Yokota, M.; Han, L. Q.; Maeda, A.; Kishida, H.; Okamoto, H.; Oshio, H. *Angew. Chem., Int. Ed.* **2005**, *44*, 6484. (b) Li, D. F.; Parkin, S.; Wang, G. B.; Yee, G. T.; Prosvirin, A. V.; Holmes, S. M. *Inorg. Chem.* **2005**, *44*, 4903. (c) Wang, S.; Zou, J. L.; Gao, S.; Song, Y.; Zhou, H. C.; Zhang, Y. Z.; You, X. Z. *J. Am. Chem. Soc.* **2004**, *126*, 8900. (d) Yoon, J. H.; Kim, H. C.; Hong, C. S. *Inorg. Chem.* **2005**, *44*, 7714. (e) Kim, J.; Han, S.; Pokhodnya, K. I.; Migliori, J. M.; Miller, J. S. *Inorg. Chem.* **2005**, *44*, 6983.

10.1021/ic052168x CCC: $33.50
Published on Web 05/25/2006

Table 1. Crystallographic Data for **1**−**5**

	1	**2**·CH_3OH·$2H_2O$	**3**·$6H_2O$	**4**	**5**
formula	$C_{84}H_{64}Cl_4Fe_2Mn_2N_{20}O_{16}$	$C_{63}H_{86}Cl_4Fe_2Mn_2N_{18}O_{27}$	$C_{60}H_{84}B_4Fe_4Mn_2N_4O_{12}$	$C_{30}H_{34}B_2Fe_2MnN_{20}O_2$	$C_3N_3Mn_{0.5}Fe_{0.5}Na$
fw	1972.91	1890.88	1934.19	895.03	156.45
cryst size (mm)	0.42 × 0.26 × 0.19	0.46 × 0.38 × 0.31	0.48 × 0.45 × 0.07	0.48 × 0.45 × 0.36	0.20 × 0.18 × 0.15
cryst syst	triclinic	monoclinic	monoclinic	monoclinic	cubic
space group	$P\bar{1}$	$P2_1/n$	$P2_1/c$	$C2/c$	$Pm\bar{3}m$
a (Å)	12.880(7)	14.035(4)	13.609(5)	27.329(4)	5.2647(7)
b (Å)	13.470(7)	16.305(5)	14.672(5)	12.4392(16)	5.2647(7)
c (Å)	13.710(7)	19.747(6)	23.230(8)	12.9051(17)	5.2647(7)
α (deg)	109.512(9)	90	90	90	90
β (deg)	99.215(9)	102.329(5)	106.857(7)	102.399(2)	90
γ (deg)	90.975(9)	90	90	90	90
vol (Å ^{3})	2207(2)	4415(2)	4439(3)	4284.7(10)	145.92(3)
Z	1	2	2	4	1
D_c (g cm^{-3})	1.485	1.422	1.447	1.387	1.780
μ (mm^{-1})	0.800	0.804	0.989	1.012	2.374
reflns collected	1006	1952	1988	1828	423
unique reflns (R_{int})	7455 (0.0311)	7721 (0.0851)	8804 (0.0389)	4195 (0.0195)	45 (0.0118)
params	623	759	578	296	9
S on F^2	1.045	1.038	1.093	1.101	1.275
R1,[a] wR2 [b] ($I > 2\sigma(I)$)	0.0741, 0.2020	0.0797, 0.1994	0.0506, 0.1239	0.0350, 0.1006	0.0115, 0.0281
R1,[a] wR2 [b] (all data)	0.1011, 0.2238	0.1438, 0.2591	0.0766, 0.1408	0.0471, 0.1092	0.0115, 0.0281

[a] $R1 = \sum||F_o| - |F_c||/\sum|F_o|$. [b] $wR2 = [\sum[w(F_o^2 - F_c^2)^2]/\sum w(F_o^2)^2]^{1/2}$. Weighting: **1**, $w = 1/[s^2(F_o)^2 + (0.1248P)^2 + 4.73P]$; **2**, $w = 1/[s^2(F_o)^2 + (0.1438P)^2 + 4.96P]$; **3**, $w = 1/[s^2(F_o)^2 + (0.0558P)^2 + 7.85P]$; **4**, $w = 1/[s^2(F_o)^2 + (0.0615P)^2 + 3.48P]$; **5**, $w = 1/[s^2(F_o)^2 + (0.0229P)^2 + 0.00P]$; where $P = [(F_o{}^2) + 2F_c^2]/3$.

semblies with higher T_c values have been structurally characterized, these include $K_{0.4}[Cr(CN)_6][Mn(S)\text{-pn}](S)\text{-pnH}_{0.6}$ ((*S*)-pn = (*S*)-1,2-diaminopropane) (T_c = 53 K),[3] $[Cu(EtOH)_2][Cu(en)]_2[Cr(CN)_6]_2$ (T_c = 57 K),[4] $Na[MnCr(CN)_6]$ (T_c = 60 K),[5] $[Mn(en)]_3[Cr(CN)_6]_2\cdot 4H_2O$ (T_c = 69 K),[6] $[Mn_2(tea)Mo(CN)_7]\cdot H_2O$ (tea = triethanolamine) (T_c = 75 K),[7] and $[Mn_2(tea)Mo(CN)_7]$ (T_c = 106 K).[7] However, structural studies on the Prussian blue family are still limited so far[5,8] because of the difficulty in growing single crystals.

Very recently, a number of cyano-bridged bimetallic magnetic assemblies containing $[M_2(CN)_4M']$ (M = Fe^{II}, Fe^{III}, W^V, M′ = Fe^{II}, Cu^{II}, Ni^{II}, Mn^{II}) square building units have been reported with various of spin-crossover,[9a] single-molecule magnetic,[9b] superparamagnetic,[9c] metamagnetic,[9d] and spin-canted antiferromagnetic[9e] behaviors. To expand the rich magnetic properties of similar cyanide-bridged bimetallic assemblies containing $[M_2(CN)_4M'_2]$ square building units with higher-spin ground states and to better understand the magnetostructural relationships of the Prussian blue family, the Mn^{II} ion was reacted with $[Fe(bipy)_2(CN)_2]^+$, $[(Tp)Fe^{III}(CN)_3]^-$, and $[Fe(CN)_6]^{3-}$ (bipy = 2,2′-bipyridine, Tp = tris(pyrazolyl)hydroborate) to synthesize a serious of $Fe^{II/III}$—Mn^{II} bimetallic complexes. Their structures and magnetic properties are investigated in this paper.

Experimental Section

Materials and General Methods. $[(bipy)_2Fe(CN)_2](ClO_4)$ and $K[(Tp)Fe(CN)_3]$ were prepared according to the literature methods.[10,11] All of the other chemicals are commercially available and were used without further purification. Elemental analyses were determined using an Elementar Vario EL elemental analyzer. The IR spectra were recorded in the 4000−400 cm^{-1} region using KBr pellets and a Bruker EQUINOX 55 spectrometer. Magnetic susceptibility data were collected with Quantum Design SQUID magnetometers MPMS XL-5 and MPMS XL-7. A correction was made for the diamagnetic contribution prior to data analysis.

Caution: Perchlorate salts of metal complexes with organic ligands are potentially explosive and should be handled in small quantities with care.

$[(bipy)_2Fe^{II}(CN)_2Mn^{II}(bipy)_2]_2(ClO_4)_4$, 1. A solution of bipy (0.063 g, 0.4 mmol) in 10 mL of methanol was added to a solution of $Mn(ClO_4)_2\cdot 6H_2O$ (0.072 g, 0.2 mmol) in 10 mL of methanol. $[(bipy)_2Fe(CN)_2](ClO_4)$ (0.104 g, 0.2 mmol) dissolved in a mixed solution of acetonitrile and methanol (1:1 v/v, 30 mL) was added to the resulting yellow solution. The mixture was stirred at 60 °C for 24 h and then cooled to room temperature. The resulting dark red solution was filtered, and the filtrate was evaporated slowly to give prism-shaped dark red crystals of **1** within two weeks. Yield: 0.104 g, 52%. Anal. Calcd for $Fe_2Mn_2C_{84}H_{68}N_{20}O_{18}Cl_4$ (**1**·$2H_2O$): C, 50.22; H, 3.41; N, 13.94. Found: C, 50.12; H, 3.64; N, 13.71. IR (KBr): ν_{CN} 2090 cm^{-1}.

$[(bipy)_2Fe^{II}(CN)_2Mn^{II}(DMF)_3(H_2O)]_2(ClO_4)_4\cdot CH_3OH\cdot 2H_2O$, 2·$CH_3OH$·$2H_2O$. A solution of $Mn(ClO_4)_2\cdot 6H_2O$ (0.036 g, 0.1 mmol) in 5 mL of DMF was added to a solution of $[(bipy)_2Fe(CN)_2](ClO_4)$ (0.057 g, 0.1 mmol) in acetonitrile and methanol (1:1 v/v, 20 mL). The resulting solution was stirred at room temperature for 2 h and then filtered. Block-shaped red crystals of **2**·CH_3OH·$2H_2O$ were obtained by diffusing diethyl ether vapor into the filtrate. Yield: 0.010 g, 11%. Anal. Calcd for $Fe_2Mn_2C_{63}H_{86}N_{18}O_{27}Cl_4$ (**2**·CH_3OH·$2H_2O$): C, 40.02; H, 4.58; N, 13.33. Found: C, 39.95; H, 4.47; N, 13.21%. IR (KBr): ν_{CN} 2088 cm^{-1}.

$\{[(Tp)Fe^{III}(CN)_3]_2Mn^{II}(DMF)_2(H_2O)\}_2\cdot 6H_2O$, 3·$6H_2O$. A solution of $Mn(ClO_4)_2\cdot 6H_2O$ (0.036 g, 0.1 mmol) in 5 mL of DMF was added to a solution of $K[(Tp)Fe(CN)_3]$ (0.077 g, 0.2 mmol) in acetonitrile and methanol (1:1 v/v, 20 mL). The resulting brown solution was stirred at room temperature for 2 h and then filtered. Slow evaporation of the filtrate gave block-shaped brown crystals of **3**·$6H_2O$ within about one month. Yield: 0.030 g, 31%. Anal. Calcd for $Fe_4Mn_2B_4C_{60}H_{84}N_{40}O_{12}$ (**3**·$6H_2O$): C, 37.26; H, 4.38; N, 28.97. Found: C, 37.10; H, 4.51; N, 28.68. IR (KBr): ν_{BH} 2528, ν_{CN} 2145 cm^{-1}.

(10) Schilt, A. A. *J. Am. Chem. Soc.* **1960**, *82*, 3000.
(11) Lescouezec, R.; Vaissermann, J.; Lloret, F.; Julve, M.; Verdaguer, M.; *Inorg. Chem.* **2002**, *41*, 5943.

Table 2. Selected Bond Distances (Å) and Angles (deg) for **1**−**5**[a]

1

Fe(1)−N(1)	1.969(5)	Fe(1)−C(21)	1.912(6)	Mn(1)−N(6)	2.237(5)	Mn(1)−N(9)	2.166(6)
Fe(1)−N(2)	2.015(5)	Fe(1)−C(22)	1.911(6)	Mn(1)−N(7)	2.249(6)	Mn(1)−N(10)	2.141(6)
Fe(1)−N(3)	2.019(5)	C(21)−N(9)	1.138(8)	Mn(1)−N(8)	2.266(5)	C(22)−N(10)#1	1.143(7)
Fe(1)−N(4)	1.980(5)	Mn(1)−N(5)	2.310(5)				
C(22)−Fe(1)−C(21)	90.2(2)	C(22)−Fe(1)−N(2)	175.6(2)	N(10)−Mn(1)−N(6)	94.6(2)	N(10)−Mn(1)−N(8)	89.1(2)
C(22)−Fe(1)−N(1)	95.6(2)	C(21)−Fe(1)−N(2)	92.2(2)	N(9)−Mn(1)−N(6)	101.42(19)	N(9)−Mn(1)−N(8)	167.4(2)
C(21)−Fe(1)−N(1)	89.0(2)	C(22)−Fe(1)−N(3)	89.3(2)	N(10)−Mn(1)−N(7)	103.8(2)	N(10)−Mn(1)−N(5)	165.9(2)
C(22)−Fe(1)−N(4)	88.3(2)	C(21)−Fe(1)−N(3)	175.8(2)	N(9)−Mn(1)−N(7)	95.5(2)	N(9)−Mn(1)−N(5)	93.64(19)
C(21)−Fe(1)−N(4)	95.7(2)	N(10)−Mn(1)−N(9)	94.4(2)				

2

Fe(1)−C(21)	1.895(6)	Fe(1)−N(3)	2.001(5)	Mn(1)−N(6)	2.189(6)	Mn(1)−O(11)	2.239(15)
Fe(1)−C(22)	1.902(6)	Fe(1)−N(4)	1.978(6)	Mn(1)−O(9)	2.227(6)	Mn(1)−O(12)	2.25(3)
Fe(1)−N(1)	2.011(5)	C(21)−N(5)	1.159(8)	Mn(1)−O(10)	2.22(2)	C(22)−N(6)#1	1.165(8)
Fe(1)−N(2)	1.970(6)	Mn(1)−N(5)	2.193(6)				
C(21)−Fe(1)−C(22)	85.9(2)	C(21)−Fe(1)−N(3)	90.8(2)	N(2)−Fe(1)−N(1)	80.9(2)	N(5)−Mn(1)−O(9)	168.5(2)
C(21)−Fe(1)−N(2)	94.3(2)	C(22)−Fe(1)−N(3)	174.1(3)	N(4)−Fe(1)−N(1)	93.7(2)	N(5)−C(21)−Fe(1)	176.4(6)
C(22)−Fe(1)−N(2)	92.0(3)	N(2)−Fe(1)−N(3)	93.2(2)	N(3)−Fe(1)−N(1)	91.8(2)	N(6)#1−C(22)−Fe(1)	174.4(5)
C(21)−Fe(1)−N(4)	91.4(2)	N(4)−Fe(1)−N(3)	81.1(2)	N(6)−Mn(1)−N(5)	97.8(2)	C(21)−N(5)−Mn(1)	153.4(5)
C(22)−Fe(1)−N(4)	94.0(3)	C(21)−Fe(1)−N(1)	174.6(3)	N(6)−Mn(1)−O(9)	93.4(2)	C(22)#1−N(6)−Mn(1)	155.9(5)
N(2)−Fe(1)−N(4)	172.0(2)	C(22)−Fe(1)−N(1)	91.9(2)				

3

Fe(1)−C(10)	1.916(5)	Fe(2)−C(23)	1.912(5)	Mn(1)−O(1)	2.135(4)	Mn(1)−N(16)	2.210(5)
Fe(1)−C(11)	1.934(6)	Fe(2)−C(24)	1.919(6)	Mn(1)−O(2)	2.151(4)	Mn(1)−N(17)#1	2.246(5)
Fe(1)−C(12)	1.931(6)	C(10)−N(7)	1.136(6)	Mn(1)−O(3)	2.215(4)	C(12)−N(9)	1.123(7)
Fe(2)−C(22)	1.928(5)	C(11)−N(8)	1.137(7)	Mn(1)−N(7)	2.202(4)		
C(10)−Fe(1)−C(12)	86.7(2)	C(12)−Fe(1)−N(2)	91.5 (2)	C(24)−Fe(2)−N(15)	92.0(2)	O(2)−Mn(1)−O(3)	173.07(16)
C(10)−Fe(1)−C(11)	86.8(2)	C(11)−Fe(1)−N(2)	91.7(2)	C(23)−Fe(2)−N(13)	92.2(2)	N(7)−Mn(1)−O(3)	91.98(17)
C(12)−Fe(1)−C(11)	88.9(2)	C(23)−Fe(2)−C(24)	87.1(2)	C(22)−Fe(2)−N(15)	92.28(19)	N(16)−Mn(1)−O(3)	85.81(18)
C(10)−Fe(1)−N(4)	92.9(2)	C(23)−Fe(2)−C(22)	85.9(2)	C(24)−Fe(2)−N(13)	179.1(2)	O(1)−Mn(1)−N(17)#1	86.05(16)
C(12)−Fe(1)−N(4)	179.1(2)	C(24)−Fe(2)−C(22)	85.1(2)	O(1)−Mn(1)−O(2)	91.22(15)	O(2)−Mn(1)−N(17)#1	87.72(17)
C(11)−Fe(1)−N(4)	90.3 (2)	C(22)−Fe(2)−N(13)	94.54(19)	O(1)−Mn(1)−N(7)	87.41(16)	N(7)−Mn(1)−N(17)#1	173.04(19)
C(10)−Fe(1)−N(6)	93.87(19)	C(23)−Fe(2)−N(11)	93.0 (2)	O(2)−Mn(1)−N(7)	94.82(16)	N(16)−Mn(1)−N(17)#1	92.64(18)
C(12)−Fe(1)−N(6)	91.6(2)	C(24)−Fe(2)−N(11)	91.9(2)	O(1)−Mn(1)−N(16)	176.04(17)	O(3)−Mn(1)−N(17)#1	85.66(18)
C(11)−Fe(1)−N(6)	179.3(2)	C(22)−Fe(2)−N(11)	176.8(2)	O(2)−Mn(1)−N(16)	92.46(18)	O(1)−Mn(1)−O(3)	90.36(16)
C(10)−Fe(1)−N(2)	177.7(2)	C(23)−Fe(2)−N(15)	178.0(2)	N(7)−Mn(1)−N(16)	93.73(17)		
O(3)···O(4)	2.814(6)	O(5)···N(17)	3.270(8)	O(6)···N(9)#2	2.843(7)	O(4)···O(6)#1	3.191(5)
O(3)···O(5)	2.828(7)	O(6)···N(18)	2.825(7)	O(4)···O(6)#3	2.771(5)	O(5)···N(18)#1	3.053(8)
O(3)−H(3B)···O(4)	169.1	O(5)−H(5B)···N(17)	148.6	O(6)−H(6B)···N(9)#2	172.4	O(4)−H(4B)···O(6)#1	131.9
O(3)−H(3A)···O(5)	175.7	O(6)−H(6A)···N(18)	166.5	O(4)−H(4A)···O(6)#3	164.0	O(5)−H(5A)···N(18)#1	168.2

4

Fe(1)−C(10)	1.918(2)	C(10)−N(7)	1.142(3)	Mn(2)−O(1)	2.1858(17)	Mn(2)−N(9)#2	2.198(2)
Fe(1)−C(11)	1.923(2)	C(11)−N(8)	1.138(3)	Mn(2)−N(7)	2.2318(19)	C(12)−N(9)	1.142(3)
Fe(1)−C(12)	1.909(2)						
C(12)−Fe(1)−C(10)	85.02(9)	C(12)−Fe(1)−N(6)	92.98(8)	O(1)−Mn(2)−N(9)#2	87.25(8)	N(9)#2−Mn(2)−N(7)	89.67(8)
C(12)−Fe(1)−C(11)	88.82(9)	C(10)−Fe(1)−N(6)	177.22(9)	O(1)#1−Mn(2)−N(9)#2	92.75(8)	N(9)#3−Mn(2)−N(7)	90.33(8)
C(10)−Fe(1)−C(11)	87.32(9)	C(11)−Fe(1)−N(6)	90.71(9)	O(1)−Mn(2)−N(9)#3	92.75(8)	O(1)−Mn(2)−N(7)#1	89.82(7)
C(12)−Fe(1)−N(2)	177.45(8)	C(12)−Fe(1)−N(4)	91.01(9)	O(1)#1−Mn(2)−N(9)#3	87.25(8)	O(1)#1−Mn(2)−N(7)#1	90.18(7)
C(10)−Fe(1)−N(2)	92.46(9)	C(10)−Fe(1)−N(4)	94.80(9)	O(1)−Mn(2)−N(7)	90.18(7)	N(9)#2−Mn(2)−N(7)#1	90.33(8)
C(11)−Fe(1)−N(2)	91.48(9)	C(11)−Fe(1)−N(4)	177.85(9)	O(1)#1−Mn(2)−N(7)	89.82(7)	N(9)#3−Mn(2)−N(7)#1	89.67(8)

5

Fe(1)−C(1)	1.96(3)	Fe(1)−C(1)#4	1.96(3)	Mn(1)−N(1)#1	2.20(2)	Mn(1)−N(1)#4	2.20(2)
Fe(1)−C(1)#1	1.96(3)	Fe(1)−C(1)#5	1.96(3)	Mn(1)−N(1)#2	2.20(2)	Mn(1)−N(1)#5	2.20(2)
Fe(1)−C(1)#2	1.96(3)	C(1)−N(1)#6	1.110(11)	Mn(1)−N(1)#3	2.20(2)	N(1)−C(1)#6	1.110(12)
Fe(1)−C(1)#3	1.96(3)	Mn(1)−N(1)	2.20(2)				

[a] Symmetry transformations used to generate equivalent atoms: **1** #1 $-x, -y+1, -z$; **2** #1 $-x+1, -y+1, -z$;. **3** #1 $-x+1, -y+1, -z+1$; #2 $x+1, y, z$; #3 $x-1, y, z$; **4** #1 $-x+1, -y+1, -z$; #2 $x, -y+1, z-1/2$; #3 $-x+1, y, -z+1/2$; **5** #1 $-y+1, -z+1-x+1$; #2 y, z, x; #3 $-x+1, -y+1, -z+1$; #4 z, x, y; #5 $-z+1, -x+1, -y+1$; #6 $-x+1, -y, -z+1$.

$\{[(Tp)Fe^{III}(CN)_3]_2Mn^{II}(DMF)_2\}_n$, 4. A solution of $Mn(ClO_4)_2 \cdot 6H_2O$ (0.036 g, 0.1 mmol) in 5 mL of DMF was added to a solution of K[(Tp)Fe(CN)$_3$] (0.077 g, 0.2 mmol) in acetonitrile and methanol (1:1 v/v, 20 mL). The resulting brown solution was stirred at room temperature for 2h and then filtered. Prism-shaped brown crystals of **4** were obtained by diffusing diethyl ether vapor into filtrate. Yield: 0.037 g, 41%. Anal. Calcd for $Fe_2MnB_2C_{30}H_{34}N_{20}O_2$: C, 40.26; H, 3.83; N, 31.30. Found: C, 40.17; H, 3.91; N, 31.26. IR (KBr): ν_{BH} 2545, ν_{CN} 2164, 2125 cm^{-1}.

$Na_2[Mn^{II}Fe^{II}(CN)_6]$, 5. In a H-tube, a solution of $K_3[Fe(CN)_6]$ (0.066 g, 0.2 mmol) in 40 mL of H_2O was slowly diffused into a mixed solution of $Mn(ClO_4)_2 \cdot 6H_2O$(0.072 g, 0.2 mmol) and

Scheme 1

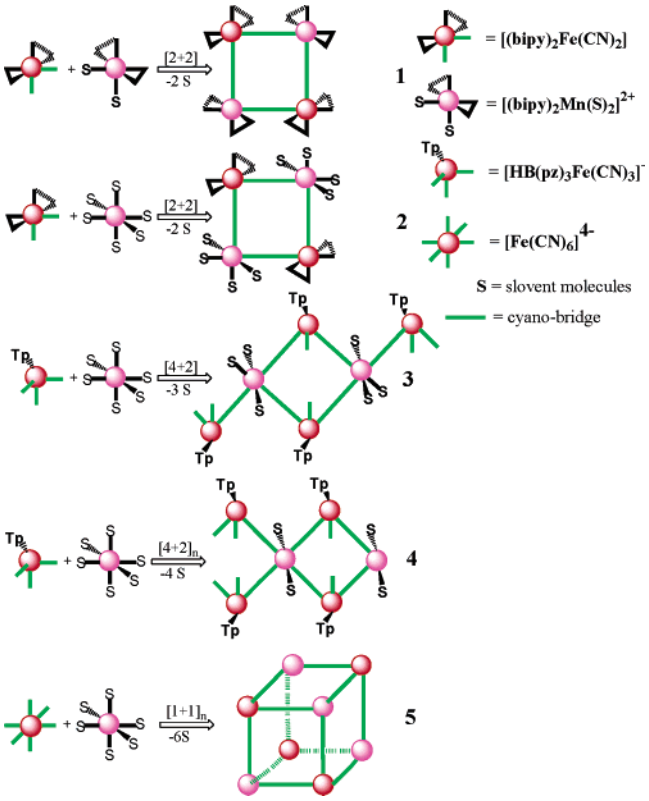

$NaClO_4 \cdot 6H_2O$ (0.046 g, 0.2 mmol) in 40 mL of water/2-propanol (5:1) to get dark brown crystals of **5**. Yield: 0.045 g, 72%. Anal. Calcd for $Na_2FeMnC_6N_6$: C, 23.03; N, 26.86. Found: C, 22.96; N, 26.97. IR (KBr): ν_{CN} 2149−2069 cm^{-1}.

X-ray Crystallography. Single-crystal data of **1**−**5** were collected at 293(2) K on a Bruker Smart 1000 CCD diffractometer with Mo Kα radiation (λ = 0.71073 Å). All empirical absorption corrections were applied with the SADABS program.[12] The structures were solved using direct methods, which yielded the positions of all non-hydrogen atoms. These were first refined isotropically and then anisotropically. All the hydrogen atoms of the ligands were placed in calculated positions with fixed isotropic thermal parameters and included in the structure factor calculations in the final stage of full-matrix least-squares refinement. The hydrogen atoms of the water molecules were located from the difference Fourier map and refined isotropically. All calculations were performed using the SHELXTL system of computer programs.[13] The crystallographic data for **1**−**5** are summarized in Table 1. The selected bond lengths and angles for **1**−**5** are listed in Table 2.

Results and Discussion

The reactions of $[(bipy)_2Fe(CN)_2](ClO_4)$ with $[Mn(bipy)_2]^{2+}$ and $[Mn(DMF)_n(H_2O)_{6-n}]^{2+}$ gave molecular squares of **1** and **2**, respectively, in which the Fe(III) ions are reduced to Fe(II) ions during the reactions, a common phenomenon found in the cyano−iron(III) compounds.[2d] Compound **1** cannot react with other linkers further since all the remaining coordination sites of Fe(II) and Mn(II) are blocked by the bipy ligand. In **2**, four coordination sites of Mn(II) are occupied by DMF and water molecules (Scheme 1), and these solvent molecules can be further substituted by other linkers. Indeed, the formation of **3** and **4** can be roughly regarded as the substitution of coordinated DMF and water molecules with $[(Tp)Fe(CN)_3]^-$ (Scheme 1). Compounds **3** and **4** can be regarded as supramolecular isomers since they possess the same molecular building blocks and different superstructures.[14] Slow diffusion of a solution of $K_3[Fe(CN)_6]$ into a solution of $Mn(ClO_4)_2 \cdot 6H_2O$ and $NaClO_4 \cdot 6H_2O$ led to the formation of **5**, in which the Fe(III) ions are also reduced to Fe(II) ions during the reaction. Compounds **1**−**4** contain the basic $[Fe_2(CN)_4Mn_2]$ square building units, while compound **5** is a 3D cubic framework analogous to that of Prussian blue.

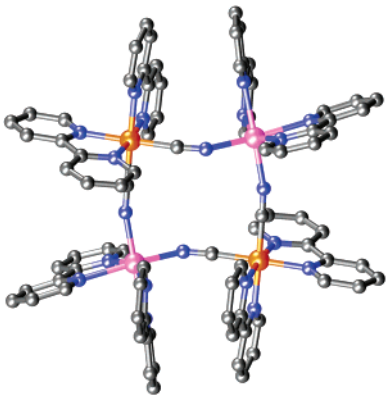

Figure 1. Structure of molecular square of **1** (pink, Mn; orange, Fe; gray, C; blue, N).

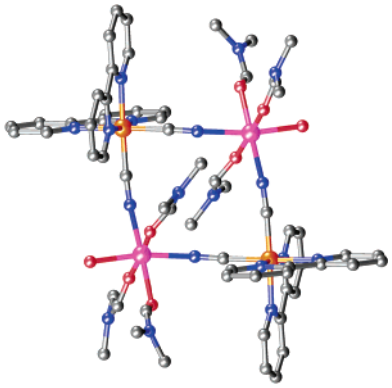

Figure 2. Structure of molecular square of **2** (red, oxygen).

Structures of Discrete Molecular Squares of 1−3. In both **1** and **2**, two $[(bipy)_2Fe^{II}(CN)_2]$ units bridge two Mn(II) through cyano bridges in the cis positions to form [2 + 2]-type discrete molecular squares (Figures 1 and 2). The remaining coordination sites of each six-coordinated Mn(II) ion are occupied by two bipy molecules in **1** and three DMF molecules and one water molecule in **2**. The Fe(II)−C(cyano) distances (1.911(6) and 1.912(6) Å in **1** and 1.895(6) and 1.902(6) Å in **2**) are shorter than the Fe(II)−N(bipy) distances (1.969(5)−2.019(5) Å in **1** and 1.970(6)−2.011-

(12) Sheldrick, G. M. *SADABS, Program for Empirical Absorption Correction of Area Detector Data*; University of Göttingen: Göttingen, Germany, 1996.

(13) Sheldrick, G. M. SHELXS 97, *Program for Crystal Structure Refinement*; University of Göttingen, Göttingen, Germany, 1997.

(14) Hennigar, T. L.; MacQuarrie, D. C.; Losier, P.; Rogers, R. D.; Zaworotko, M. J. *Angew. Chem., Int. Ed. Engl.* **1997**, *36*, 972. (b) Moulton, B.; Zaworotko, M. J. *Chem. Rev.* **2001**, *101*, 1629.

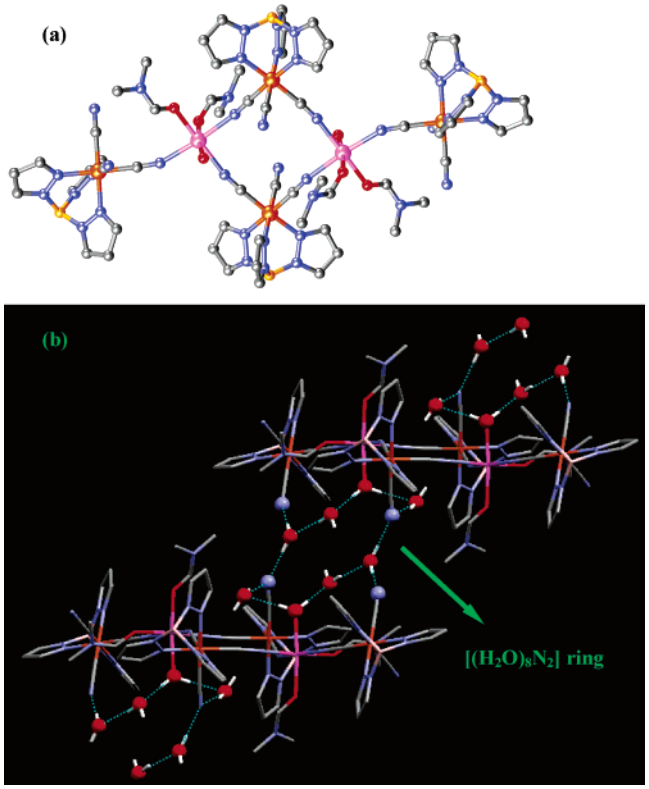

Figure 3. (a) Structure of molecular square of **3**. (b) The $[(H_2O)_8N_2]$ ring between two adjacent Fe_4Mn_2 molecules (yellow, B).

(5) Å in **2**), and they are all shorter than the Mn−N distances (2.141(6)−2.310(5) Å in **1** and 2.189(6)−2.193(6) Å in **2**). The $Fe^{II}\cdots Mn^{II}$ separations are 4.946 and 5.183 Å in **1** and 5.090 and 5.112 Å in **2**.

In **1**, there are weak intermolecular $\pi\cdots\pi$ interactions between two adjacent bipy molecules coordinated to Mn(II), resulting in a 1D chainlike structure (Figure S1) with a centroid···centroid distance between the two bipy planes of 3.54 Å. In **2**, there are also weak intermolecular $\pi\cdots\pi$ interactions between two adjacent bipy molecules coordinated to Fe(II) to generate a 2D sheet (Figure S2a) with the centroid···centroid distance between the two bipy planes being 3.87 Å. The 2D sheets are further connected through the intermolecular hydrogen bonds of $Mn-OH_2\cdots OH_2\cdots MeOH\cdots OH_2\cdots OH_2-Mn$ to form 3D structures (Figure S2b) with O(9)···O(13) and O(13)···O(14) distances of 2.415 and 3.018 Å, respectively.

The structure of **3** is a neutral Fe_4Mn_2 hexanuclear cluster (Figure 3a), in which two $[(Tp)Fe^{III}(CN)_3]^-$ anions act as bidentate ligands to bridge two Mn(II) ions through cyano bridges in the cis positions to construct a molecular square of $[Fe_2Mn_2(CN)_4]^{6+}$. The remaining coordination sites of each six-coordinated Mn(II) ion are occupied by one monodentate $[(Tp)Fe^{III}(CN)_3]^-$ anion, two DMF molecules, and one water molecule. The intramolecular $Fe^{III}\cdots Mn^{II}$ separations of 5.116−5.240 Å are close to the $Fe^{II}\cdots Mn^{II}$ separations in **1** and **2**.

Each discrete Fe_4Mn_2 molecule is linked to two adjacent Fe_4Mn_2 molecules through the hydrogen-bonding interactions of the novel $[(H_2O)_8N_2]$ rings to generate a 1D neutral molecular strap (Figure 3b). The 1D hydrogen-bonded straps

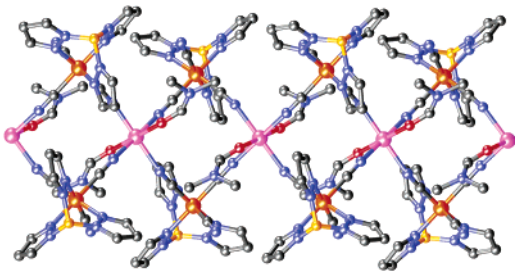

Figure 4. 1D double zigzag chain of **4**.

are further packed along the *a* axis through the intermolecular hydrophobic interactions of the Tp molecules to form a 3D structure (Figure 3S).

1D Chain Structure of 4. In **4**, each bidentate $[(Tp)Fe^{III}(CN)_3]^-$ anion bridges two Mn(II) ions to generate a neutral cyanide-bridged double-zigzag −Fe(III)−CN−Mn(II)−NC− chain (Figure 4). Within the chain, the basic building unit is a $Mn_2(CN)_4Fe_2$ square with each Mn(II) shared by two adjacent squares. Each Mn(II) ion in the chain is coordinated with two nitrogen atoms of two individual $[(Tp)Fe^{III}(CN)_3]^-$ units, two oxygen atoms of DMF molecules in the equatorial plane, and two nitrogen atoms of two $[(Tp)Fe^{III}(CN)_3]^-$ units in the axial positions. The axial Mn−N distances (2.232(2) Å) are slightly longer than the equatorial Mn−N and Mn−O distances (2.186(2) and 2.198(2) Å). The $Fe^{III}\cdots Mn^{II}$ separations are 5.109 and 5.183 Å, respectively. The 1D chains are held togther through intermolecular $\pi\cdots\pi$ interactions between the two adjacent pz rings (Figure S4), with the centroid···centroid distance and dihedral angle between each pair of rings being 3.75 Å and 0.0°, respectively.

It's interesting to note that the solvent molecules coordinated to the Mn(II) ions are DMF and water in **2** and **3**, while only DMF molecules are coordinated to Mn(II) in **4**. Usually, the DMF molecule shows a stronger coordination ability to metal ions than the water molecule, so DMF coordination occurs prior to coordination with metal ions. The presence of coordinated water molecules in **2** and **3** is the prerequisite for the formation of intermolecular hydrogen bonds (see Figures S2b and 3b).

3D Cubic Structure of 5. The structure of **5** shows a 3D cubic framework (Figure 5) analogous to that of Prussian blue. Each unit cell contains one-half of an $Na_2[MnFe(CN)_6]$ molecule, so that the Mn and Fe atoms are not distinguishable and each atom occupies half of the position. The C and N atoms of the bridging CN ions are disordered so that C and N are not distinguishable either, and each atom appears to be 0.5 C/0.5 N. Each $[Fe(CN)_6]^{4-}$ connects to six Mn atoms through cyano bridges. Both Mn and Fe atoms locate in the cubic body center, and the Na atoms locate in the eight apexes and occupy the vacancy volume of the 3D cubic framework. The shortest $Fe^{II}\cdots Fe^{II}$ and $Mn^{II}\cdots Mn^{II}$ separations (10.529 Å) in **5** are slightly longer than the $Fe^{II}\cdots Fe^{II}$ and $Fe^{III}\cdots Fe^{III}$ separations of 10.166 Å in Prussian blue ($Fe_4[Fe(CN)_6]_3\cdot xH_2O$). In **5**, the basic building unit can also be regarded as being a $Mn_2(CN)_4Fe_2$ square, and the connections of $Mn_2(CN)_4Fe_2$ squares via sharing of their vertexes along three dimensions give the 3D framework of **5**. Although the

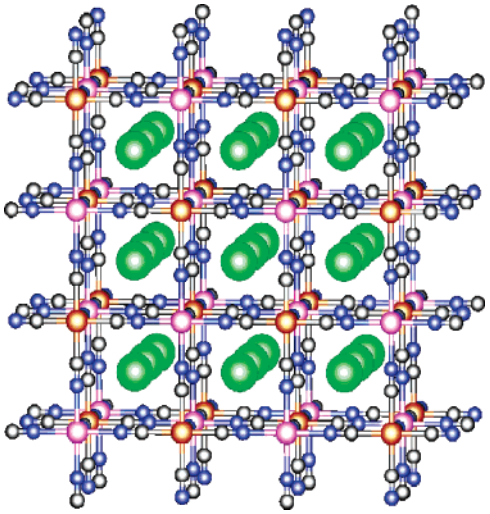

Figure 5. 3D cubic framework of **5** (green, Na).

structure of Prussian blue, $Fe_4[Fe(CN)_6]_3 \cdot xH_2O$, was determined by powder X-ray diffraction analysis twenty years ago,[15] its single-crystal structure has not yet been determined because of the difficulty in growing single crystals. The composition of **5** is almost identical to that of the reduced product of Prussian blue, Everitt's salt of $K_2[Fe_2^{II}Fe^{II}(CN)_6]$, and to the best of our knowledge, the structure of **5** is the most analogous to that of Prussian blue.

Magnetic Properties of 1−5. The magnetic properties of **1** and **2** are shown in Figure 6 in the form of $\chi_M T$ versus T plots. The μ_{eff} values at room temperature, 8.49 μ_B for **1** and 8.38 μ_B for **2**, are close to the spin-only value of 8.37 μ_B expected for two uncoupled Mn(II) ions ($S = 5/2$, $g = 2.0$). The $\chi_M T$ values, in the 300−20 K temperature range, remain practically constant with decreasing temperature at 9.01−9.05 $cm^3\ mol^{-1}\ K$ for **1** and 8.77−8.78 $cm^3\ mol^{-1}\ K$ for **2**; then they increase rapidly to 10.04 $cm^3\ mol^{-1}\ K$ for **1** and 10.06 $cm^3\ mol^{-1}\ K$ for **2** at 2.0 K. The plots of $1/\chi_M$ versus T (Figure S5) in the whole temperature range obey the Curie−Weiss law with small positive Weiss constants of $\Theta = 0.15$ K for **1** and 0.13 K for **2**. These observations suggest very weak ferromagnetic interactions between the two high-spin Mn(II) ions through the bent −NC−Fe−CN− bridges. The field dependence of magnetization curves of **1** and **2** (Figure S6) show a linear increase with applied field in the low-field range and rapid saturation. The saturation magnetizations, M_s, of 10.04 μ_B for **1** and 9.96 μ_B for **2**, are very close to the expected value of 10 μ_B, adding support for the assumption that the two HS Mn(II) ions in **1** and **2** are ferromagnetically coupled. The magnetic susceptibility data were fitted using the following equation with $H = -2JS_1S_2$:[16]

$$\chi_M = \frac{2N\beta^2 g^2}{kT} \times \frac{\exp(x) + 5\exp(3x) + 14\exp(6x) + 30\exp(10x) + 55\exp(15x)}{1 + 3\exp(x) + 5\exp(3x) + 7\exp(6x) + 9\exp(10x) + 11\exp(15x)} + \mathrm{TIP}$$

with

$$x = 2J/kT$$

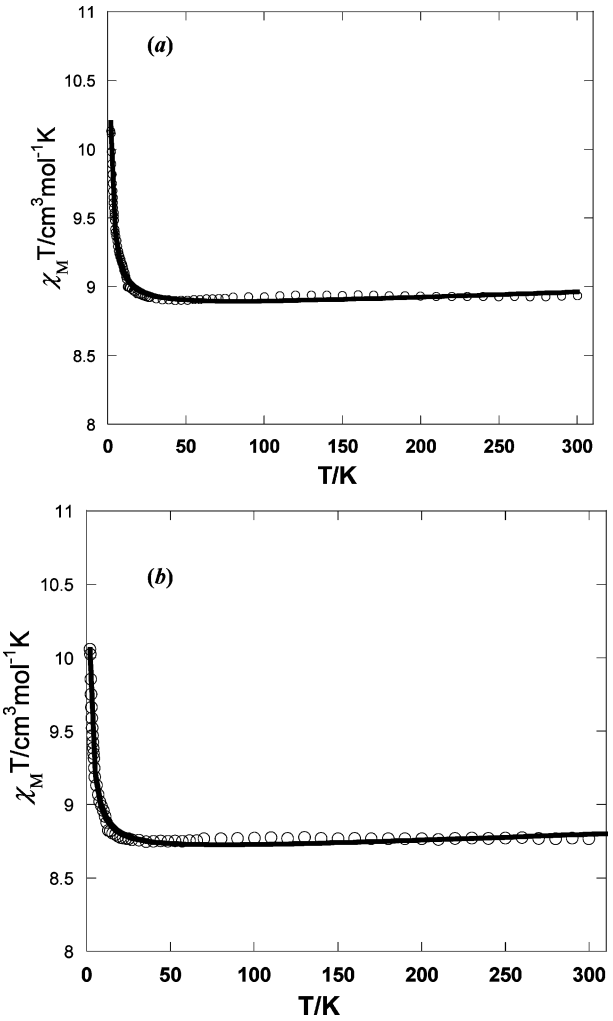

Figure 6. Temperature dependence of $\chi_M T$ vs T for (a) **1** and (b) **2** measured at 1 kOe. The solid lines are the best-fit curves.

where the symbols have their usual meaning. J is the exchange coupling parameter, and TIP represents metallic impurities. Least-squares fittings of all experimental points lead to $g = 2.01$, $J = 0.038\ cm^{-1}$, and TIP $= 4.22 \times 10^{-4}$ with a correlation coefficient of 0.99681 for **1** and $g = 1.99$, $J = 0.040\ cm^{-1}$, and TIP $= 4.46 \times 10^{-4}$ with a correlation coefficient of 0.99653 for **2**. The above similar magnetic behaviors of **1** and **2** correspond to their similar structures.

The magnetic properties of **3** and **4** are shown in Figure 7. The $\chi_M T$ values at room temperature, 9.92 $cm^3\ K\ mol^{-1}$ (8.91 μ_B) per Fe_4Mn_2 unit for **3** and 5.37 $cm^3\ K\ mol^{-1}$ (6.55 μ_B) per Fe_2Mn unit for **4**, are very close to the expected values of 9.06 μ_B for **3** and 6.40 μ_B for **4**, for the uncoupled LS Fe(III) ions ($S = 1/2$, $g = 2.0$) and HS Mn(II) ions ($S = 5/2$, $g = 2.0$). The $\chi_M T$ values decrease slowly with decreasing temperature to 9.11 $cm^3\ mol^{-1}\ K$ at 58 K for **3** and 4.75 $cm^3\ mol^{-1}\ K$ at 60 K for **4**; then they decrease rapidly to 1.85 $cm^3\ mol^{-1}\ K$ at 2.0 K for **3** and 0.50 $cm^3\ mol^{-1}\ K$ at 1.9 K for **4**. The plots of $1/\chi_M$ versus T in the 20−300 K temperature range obey the Curie−Weiss law with negative

(15) Buser, H. J.; Schwarzenbach, D.; Petter, W.; Ludi, A. *Inorg. Chem.* **1977**, *16*, 2704. (b) Herren, F.; Fischer, P.; Ludi, A.; Hälg, W. *Inorg. Chem.* **1980**, *19*, 956.

(16) Kahn, O. *Molecular Magnetism*; VCH Press: New York, 1993; p 114.

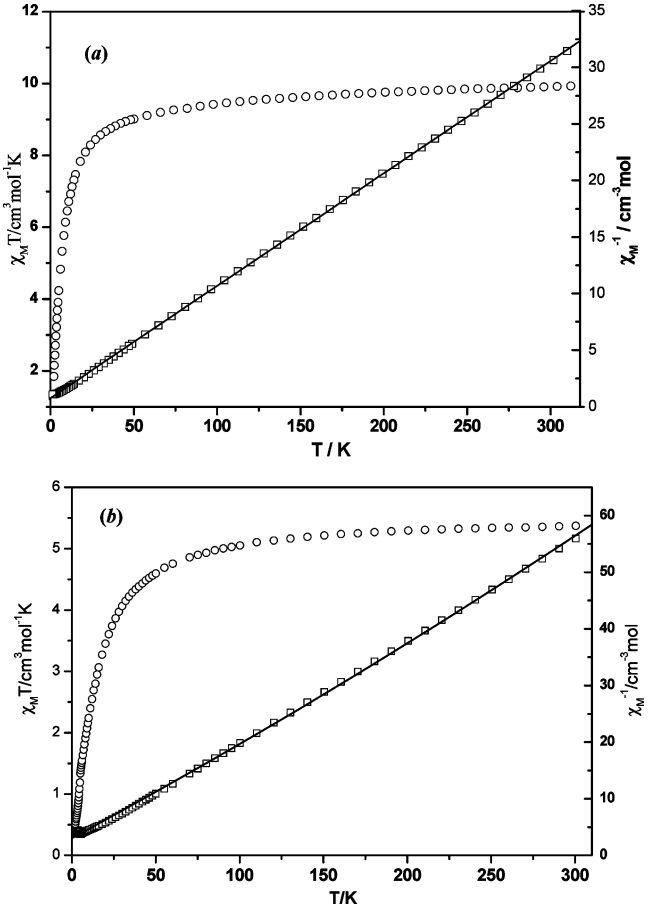

Figure 7. Temperature dependence of $\chi_M T$ (○) and $1/\chi_M$ (□) for (a) **3** and (b) **4** measured at 1 kOe.

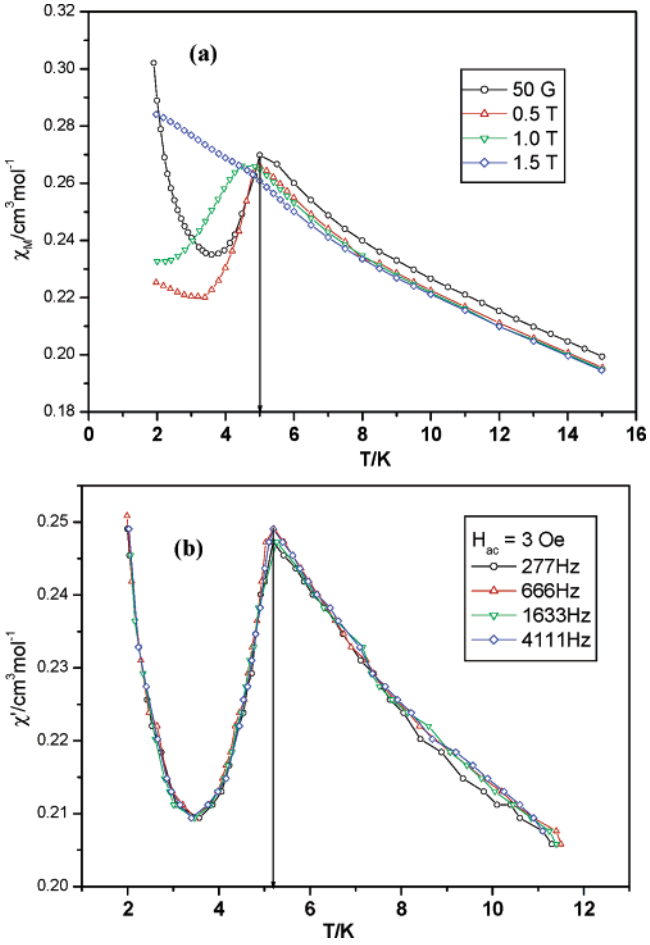

Figure 8. Temperature dependence of (a) dc χ_M at different applied fields and (b) the in-phase χ' at different frequencies for **4**.

Weiss constants of $\Theta = -6.53$ K for **3** and $\Theta = -15.8$ K for **4**. These observations suggest weak antiferromagnetic (AF) interactions between the Fe(III) and Mn(II) ions through the cyan bridges, and the smaller Weiss constant for **3** suggests that the AF coupling in **3** is weaker than that in **4**.

A metamagnetic-like behavior is observed from the temperature dependence of the dc and ac susceptibility measurements, as shown in Figure 8a and b, respectively. At lower dc fields, the χ_M versus T plots display peaks at 5.0 (0.05 and 5 kOe) and 4.5 K (10 kOe), which disappear at a higher dc field (15 kOe). At zero dc field and 3 Oe alternating current (ac) field, the in-phase of χ' versus T plots at 277, 666, 1633, and 4111 Hz also display maximums at 5.2 K. While the out of phase of χ'' values are close to zero. This clearly demonstrates that compound **4** has an antiferromagnetic state below a Néel temperature (T_N) of 5.2 K, based on the positions of the peaks. The metamagnetic-like behavior is also confirmed by the field dependence of the magnetization measurement at 1.9 K (Figure 9 and the inset of Figure 9). The magnetization curve displays an explicit sigmoidal shape, with a critical field, H_c, of 10.5 kOe from the peak position of the dM/dT versus H curve (the inset of Figure 9). The magnetization value of 2.2 μ_B at 50 kOe is less than the expected value of 3 μ_B ($S_T = 5/2 - 1 = 3/2$ for the Fe_2Mn unit), indicating an incomplete saturation at 50 kOe. It's interesting to note that compound **4** shows metamagnetic-like behavior, while compound **3** does not. The

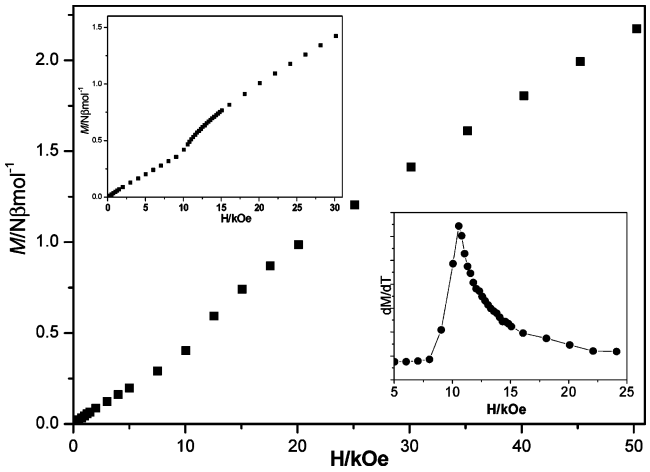

Figure 9. Field dependence of the magnetization of **4** at 2.0 K. The insets are the plots of M vs H and dM/dT vs H (the solid line is guide).

magnetic properties of **4** can be rationalized on the basis of its structure. As shown in Scheme 2, the AF couplings between the Fe(III) and Mn(II) ions through the cyano bridges within the chain lead to a ferrimagnetic chain. At lower fields, the AF interactions between the adjacent chains result in an AF ground state, which becomes a ferrimagnetic or spin-polarized state at higher fields.[17]

The magnetic properties of **5** are shown in Figure 10. The $\chi_M T$ value at room temperature, 4.62 cm^3 K mol^{-1} (6.08 μ_B)

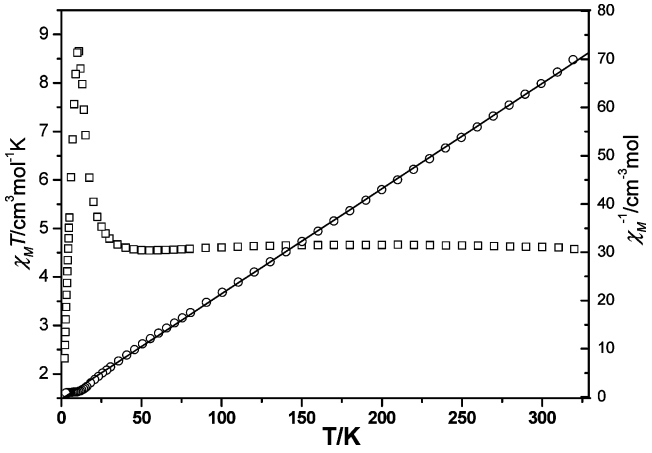

Figure 10. Temperature dependence of $\chi_M T$ (□) and $1/\chi_M$ (○) for **5** measured at 1 kOe.

Scheme 2

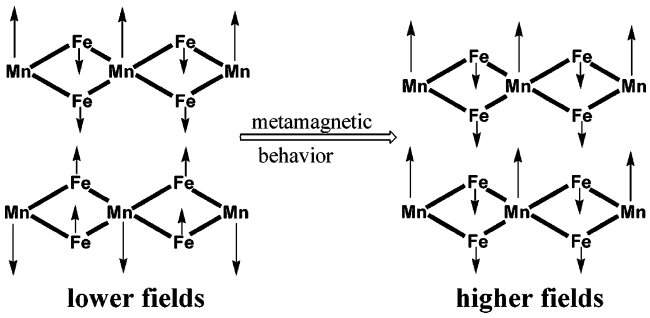

per MnFe unit, is close to the expected value of 5.92 μ_B for one HS Mn(II) ions ($S = 5/2$, $g = 2.0$). Similar to that for compound **1**, the $\chi_M T$ value remains constant with decreasing temperature until 40 K; then it increases sharply to a maximum value of 8.65 cm^3 mol^{-1} K (8.32 μ_B) at 11 K, and then it decreases below this temperature. The plot of $1/\chi_M$ versus T in the 40−320 K temperature range obeys the Curie−Weiss law with a positive Weiss constant of $\Theta = 1.2$ K. The abrupt increase in $\chi_M T$ around 11 K suggests the onset of 3D magnetic ordering. Susceptibility measurements of the ac type confirm the ferromagnetic ordering below 3.5 K (Figure 11) and reveal no significant frequency dependence. The onset of 3D magnetic ordering can be attributed to the nature of the ferromagnetic interaction of two Mn(II) ions in the basic building unit of $[Fe_2(CN)_4Mn_2]$. According to Néel's molecular field theory, for Prussian blue analogues $M'[M(CN)_6]_y$, the relationship between the critical temperature, T_c, and the magnetic exchange integral, J, is expressed as[18]

$$2kT_c \approx |J|(y)^{3/2}[n_M(n_M + 2)n_{M'}(n_{M'} + 2)]^{1/2}$$

where n_M and $n_{M'}$ are the number of unpaired electrons in the metal ions M and M′. With a T_c value of 3.5 K for **5**, the $|J|$ value is estimated to be 0.035 cm^{-1}, which is close to the J values of 0.038 and 0.040 cm^{-1} for **1** and **2**, respectively.

(17) Zhang, Y. Z.; Gao, S.; Sun, H. L.; Su, G.; Wang, Z. M.; Zhang, S. W. *Chem. Comm.* **2004**, 1906. (b) Zhang, Y. Z.; Gao, S.; Wang, Z. M.; Su, G.; Sun, H. L.; Pan, F. *Inorg. Chem.* **2005**, *44*, 4534.

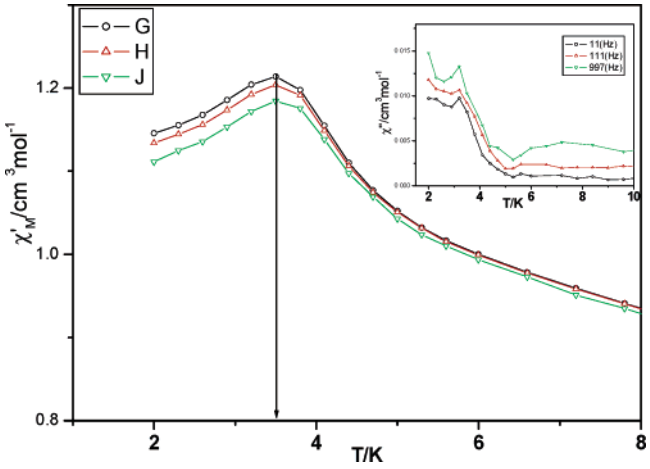

Figure 11. Temperature dependence of the in-phase χ' and out-of-phase χ'' (inset) at different frequencies for **5**.

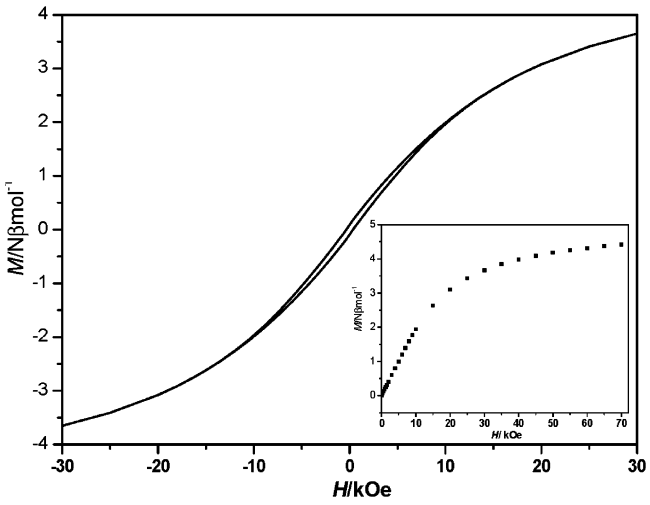

Figure 12. Hysteresis loop for **5** at 2 K. The inset shows the field dependence of the magnetization at 2.0 K.

The field dependence of magnetization at 2 K (Figure 12, inset) shows a gradual increase with a value of 4.4 μ_B at 70 kOe, which is slightly less than the expected value of 5.0 μ_B. Hysteresis loops have been observed at 2 K (Figure 12) with a remnant magnetization of 503 cm^3 Oe mol^{-1} and a coercive field, H_c, of 330 G.

In summary, five cyano-bridged Fe−Mn complexes, three discrete molecular squares, one 1D double-zigzag chain, and one 3D cubic framework analogous to that of Prussian blue, were successfully synthesized. Compounds **1**, **2**, and **5** possess similar $[Fe^{II}_2(CN)_4Mn^{II}_2]$ square building units, and the adjacent Mn(II) ions are ferromagnetically coupled through the −NC−Fe(II)−CN− bridges. Compound **3** shows a discrete Fe_4Mn_2 square with weak antiferromagnetic coupling between the Fe(III) and Mn(II) ions. Compound **4** contains the basic building unit of the $Fe^{III}_2(CN)_4Mn^{II}$ square, which shows a metamagnetic-like behavior with $T_N = 5.2$ K and $H_c = 10.5$ kOe.

(18) Ferlay, S.; Mallah, T,; Ouahès, R.; Veillet, P.; Verdaguer, M. *Inorg. Chem.* **1999**, *38*, 229.

Acknowledgment. This work was supported by the NSFC (20371051, 20221101, 20490210) and NSF of Guangdong Province (04205405).

Supporting Information Available: X-ray crystallographic data for **1**−**5** in CIF format, structural figures for **1**−**4**, temperature dependence of $1/\chi_M$, and field dependence of the magnetization for **1** and **2** (PDF). This material is available free of charge via the Internet at http://pubs.acs.org.

IC052168X